Applied Mathematics & Information Sciences
An International Journal

http://dx.doi.org/10.12785/amis/092L25

Head Pose and Gaze Direction Tracking for Detecting a Drowsy Driver

*In-Ho Choi and Yong-Guk Kim**

Department of Computer Eng. Sejong University, Kwangjin-Gu, Seoul, Korea

Received: 4 Jun. 2014, Revised: 2 Aug. 2014, Accepted: 3 Aug. 2014
Published online: 1 Apr. 2015

Abstract: This paper proposes a new drowsy-driver detection system that uses the head-pose, gaze direction and eye-blinking states of a driving person. Head-pose of the driver is estimated by using optical flow of the facial features, which are acquired with a corner detection algorithm. To estimate the gaze direction of the driver, we trace the center point of the pupil. The eye-blinking is estimated by using the Integral Projection Function (IPF). Then the level of drowsiness is calculated by combining these three parameters in a data fusion method. Performance of the system is evaluated using the new driver database. Result suggests that the system has a practical potential for detecting drowsiness of the drivers.

Keywords: Driver Drowsiness Detection, Gaze Direction, Eye Blinking, Head Pose Estimation

1 Introduction

The major categories of car accidents are divided into distraction and drowsiness of drivers. Drowsy driving refers to when a driver is half-sleeping after a long period of driving. Currently, more than 30% of deaths caused by car accidents are attributed to drowsy driving. In 2008, National Highway Traffic Safety Administration (NHTSA) estimates that 100 000 police reports on vehicle crashes were direct outcomes of driver drowsiness resulting in 1550 deaths, 71 000 injuries, and $12.5 billion in monetary losses [1]. For that reason, car manufacturers in the world are eagerly developing a system that can prevent drowsy driving.

Head pose estimation is a good index that directly shows the current state of the driver. When drowsy, a personś head is leaned forward due to the weight of the head. However, then, it becomes difficult to breath and the head tries to regain the normal state, which results in nodding. Head pose estimation has been developed into POSIT (Pose from Orthography and Scaling with ITerations) algorithm [2]. The relationship between a 3D object and 2D feature can be estimated. However, it was difficult to build a continuous relationship among objects. Meanwhile, La Cascia et al [3] estimated the head pose with a cylinder model using a texure-map method. Though it runs fast, there was a problem with the real-time use due to its low accuracy. Therefore, we adopted the POSIT plus auto reinitialization method [4], which is a model suitable for the real time case because it can reinitialize in a fast and automatic way.

Gaze detection is widely used not only for drowsiness prevention systems but also for other areas including marketing, psychology, and Human Computer Interaction. For instance, in marketing, peopleś level of interest can be measured by the time during which they directly look at a product. Already, large retailers have used for a system that decides product arrangement and sales. However, this kind of systems requires high maintenance costs. Moreover, gaze detection is actively used as study user interface in HCI research area. Gaze is used to control a computer mouse or for people with disabilities to communicate. However, there are problems with its accuracy and eye fatigue.

The direction of gaze can be recognized by observing pupil of the eye. Since the position of the pupilś center indicates the gaze direction. Pupil center detection includes the appearance-based method and feature-based method. The other approach would be using AdaBoost algorithm which requires an extensive training using a lot of pupil images [5]. It allows eye-tracking even with eyeglasses. However, it is not fast and the result varies according to the training data. On the other hand, the feature-based method is based on IPF (Integral Projection

* Corresponding author e-mail: ykim@sejong.ac.kr

© 2015 NSP
Natural Sciences Publishing Cor.

Samsara EX1036
Samsara v. Motive
IPR2026-00108

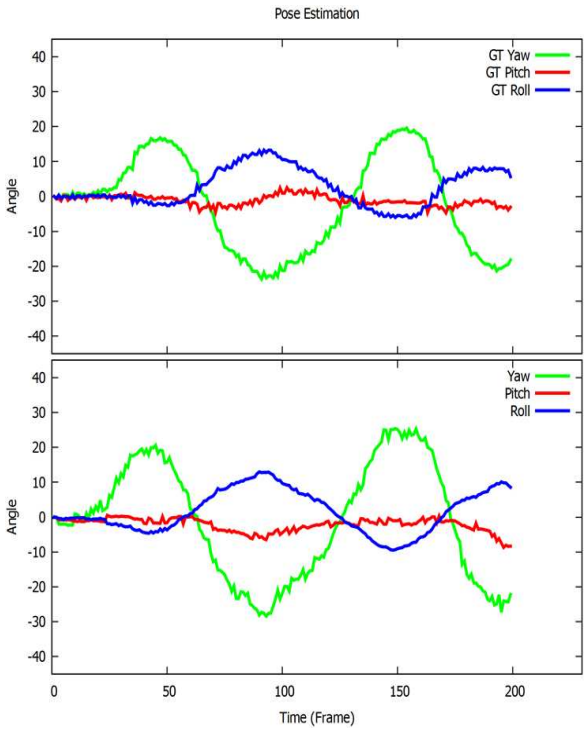

Fig. 1: Head-pose estimation result for 200 frames (Top: The Ground Truth, Down: Estimated Values)

Function) [6], which finds the center point by projecting features into X and Y axes. It is known that it has higher accuracy than the appearance-based method, but the problem is the processing time. In this study, we have used the feature-based method that uses CDF (Cumulative Distribution Function) [7]. Although it does not allow tracking with eyeglasses, it was suitable for real-time processing because of its fast speed.

The other popular way to estimate drowsiness of driver is to measure the eye closure, called PERCLOS (PERcentage of eyelid CLOSure) over a certain time period. This method plays an important role in detecting drowsiness to be declared by NHTSA and US Department of Transportation as ẗhe most reliable and valid bio-physiological determinant of a driverś alertness level.ẗ At present, NHTSA continues to evaluate the performance of driver drowsiness detection using PERCLOS. It can carry out the evaluation with various lighting conditions and diverse environments for a variety of vehicle interiors. However, sunglasses worn by most drivers are the biggest problem of the PERCLOS method. To this end, the method of sending very strong IR (Infra-Red) light and shooting it with the infrared camera is often used. Because sunglasses block visible light but transmits IR. However, the use of very strong IR may cause skin cancer, tumor, blood cancer etc. in the human body. In addition, streetlights and street trees of the driver environment may lead to lighting changes and obstruction on the driverś face. For instance, Wierwille [8] used PERCLOS based on the increase of blinking. It determines drowsiness by calculating the proportion of blinking with a certain time period. Also, drowsiness can be determined based on the opening of mouth using BPNN (back propagation neural networks), which was introduced by Wang [9].

This study proposes a system that directly determines the driverś state using a camera, which is a non-contacting sensor. The drowsiness of a driver is determined by combining the gaze direction and eye blinking, and head pose estimation in term of data fusion method.

2 Head Pose Estimation

We aim to calculate rotation vector of 3D in a 2D image while automatically performing initialization without training. To do so, a face with 3D coordinate, instead of 2D, has been created to increase its accuracy. It is based on an average 3D face model created by using FaceGen [10]. To estimate head pose, POSIT algorithm is adopted to measure the rotation of a 3D object. The test result is evaluated by using the Boston Database(see Table 1.).

2.1 Head Pose Estimation

The purpose of head pose estimation is to calculate the rotation vector of the face in the current image. Here, the rotation vector corresponds to nodding(X axis), shaking(Y axis), and tilting (Z axis). Equation 1 shows rotation vector.

$$\begin{aligned} R &= R_z(\varphi)R_y(\theta)R_x(\gamma) \\ Where(\varphi,\theta,\gamma) &= (Tilting, Shaking, Nodding) \end{aligned} \tag{1}$$

To calculate the rotation vector above, 30-40 feature points for tracking will be extracted from a 2D image, which was acquired at first. For feature extraction, Corner detection and KLT (Kanade-Lucas-Tomasi) feature tracker are used. Alignment is performed based on the

Table 1: Head-pose estimation results using Boston DB

(φ, θ, γ)=(Tilting, Shaking,Nodding)

(5.976,-22.104, -0.461)	(1.274,-3.933,-18.786)	(28.959,9.492,4.460)
(7.054,-22.774,-3.508)	(0.994,-3.381,-21.014)	(31.489,7.213,8.010)

(Top: The Ground Truth, Down: Estimated Values)

© 2015 NSP
Natural Sciences Publishing Cor.

pupil positions in the current face and the 3D average model. And then, assuming that the 2D image face and 3D model correspond one-to-one, initialization is performed to the 3D coordinate that corresponds to the extracted feature points.

Motion tracking is performed regarding the feature point extracted for the second time. We use the optical flow among various motion tacking methods because it has high tracking speed and accuracy. Motion vector is calculated based on feature point. Later, optical flow looks for a vector whose motion vector is the same but only the position has been moved by designating a certain block.

Third, the rotation is calculated by using the initialized standard 3D coordinate and current 2D coordinate. Here, the POSIT algorithm is used to obtain the rotation. POSIT calculates rotation and translation based on the correlation between points on the 2D and corresponding points on the 3D. Equation 2 is the formula of POSIT.

$$s\begin{bmatrix} u \\ v \\ 1 \end{bmatrix} = \begin{bmatrix} f_x & 0 & c_x \\ 0 & f_y & c_y \\ 0 & 0 & 1 \end{bmatrix} \begin{bmatrix} r_{11} & r_{12} & r_{13} & t_1 \\ r_{21} & r_{22} & r_{23} & t_2 \\ r_{31} & r_{32} & r_{33} & t_3 \end{bmatrix} \begin{bmatrix} X \\ Y \\ Z \\ 1 \end{bmatrix} \tag{2}$$

In this formula, (X,Y,Z) represents the coordinate of 3D and (u,v) that of 2D, which is obtained based on projection. Camera Matrix has intrinsic parameters, which are the center points of image, (c_x,c_y); scale factor (s), and focal length between pixels (f_x, f_y). The rotation matrix and translation matrix, $[R|t]$, are extrinsic parameters that have r_{ij} and t_{ij}. POSIT algorithm estimates the rotation matrix and translation matrix on the 3D.

As input data of POSIT, the feature coordinate of 2D that corresponds to the 3D object is received, and these are the 3D standard model coordinate and feature point extracted from the 2D image. With the obtained rotation matrix as the determinant, rotation vector corresponding to three axes is calculated.

2.2 Head Pose Estimation Result

We used the public database of Boston University to evaluate the estimation of head pose [2](see Table 2). The database consists of 72 videos of 200 frames and uniform and varying lights. Each video has exactly calculated rotation and translation vector by installing magnetic sensors on the head. Table 1 shows the exact ground truth values in database and our estimation result. Each rotation vector is shown as (φ, θ, γ). Fig. 1 is the rotation vector graph regarding the 200 frames of the video. Next, to obtain exact estimation error, we calculated the MAE (Average Mean Absolute Error) for the entire 200 frames. Equation 3 shows MAE.

Table 2: MAE for the data of Fig. 1

	Tilting	Shaking	Nodding
MAE	1.467	1.856	3.992

$$MAE = \frac{1}{N}\sum_{i=1}^{N}\left|\theta_i - \widehat{\theta}_i\right| \tag{3}$$

Here, N refers to the entire frames and $\theta_i, \widehat{\theta}_i$ ground truth and estimation respectively. Table 2 shows the MAE result of the above graph shown in Fig. 1.

As shown in the table 2 there is high accuracy with the estimated result of the head pose. Based on this accuracy, drowsiness is determined when the change in nodding is 30 or bigger in a short period.

3 Gaze Direction and Blink Detection

Human eyes move very rapidly and the gaze direction varies widely. We track the gaze direction based on the vertical and horizontal movement of the eye. The direction tracking begins from finding the center of the pupils. We use the pupil center detection based on the CDF (Cumulative Distribution Function). Fig. 2 illustrates a flowchart of carrying out the pupil center detection task using the CDF. By using the detected points, the average distance between the eyes on the current face will be measured to find an error.

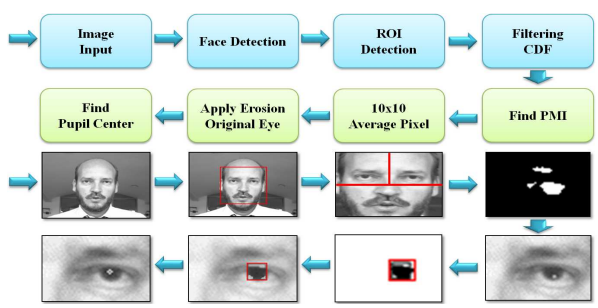

Fig. 2: Flowchart of the Pupil Center Detection System using CDF

3.1 Pupil Center Detection using CDF

Since the gaze direction has to be detected in the real time, we have adopted the pupil center detection based on CDF analysis, which is fast and highly accurate in doing the calculation. First, we apply AdaBoost algorithm to detect the eye area within the input image. Then, we designate

© 2015 NSP
Natural Sciences Publishing Cor.

the top right and left, where the pupils are located, as ROI (Region of Interest). The distribution map is created based on the CDF analysis of the designated ROI. Equation 4 shows the result.

$$CDF(r) = \sum_{w=0}^{r} P(w) \quad where = 0 \leq w \leq 255 \tag{4}$$

Here, $P(w)$ represents the histogram of the gray level and r the total size of it, which equals the width of the image multiplied by the height. The CDF distribution map is generated by accumulation of brightness of ROI. Most of the human pupils have darker color than the skin, and the sclera is always white. Based on this fact, the section until 0.05 on the distribution map is extracted as a preliminary pupil region.

$$I'(x,y) = \begin{Bmatrix} 255 & CDF(I(x,y) \leq 0.05 \\ 0 & Otherwise \end{Bmatrix} \tag{5}$$

Using equation 5 the preliminary pupil region is extracted as white, including the pupil, eyebrow, and eyelid. The preliminary region does not detect the exact center of the pupil, because the detection rate changes according to the light reflected on the pupil and different pupil colors can produce different result.

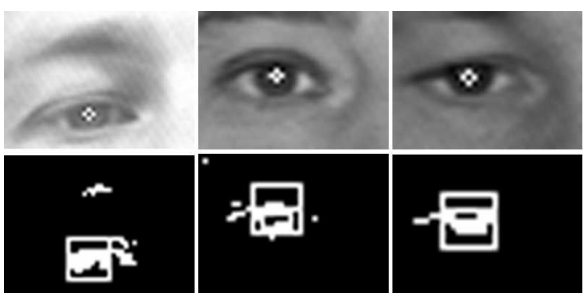

Fig. 3: Pupil Center Detection using CDF. Each eye area and the detected center(Top); ROI is indicated as a square over a CDF image(Bottom).

Later, for exact pupil center detection, PMI (Pixel with the Minimum Intensity) is extracted from ROI and compared. From the center of the extracted PMI, 1010 region is designated and the CDF analysis result is accumulated to calculate the exact center of the pupil. Fig. 3 shows the result of pupil center detection using CDF.

To determine the accuracy of the algorithm, BioID DB[5] is used and the accuracy of pupil center detection is tested using equation 6.

$$D_{eye} = \frac{max\left(\| Cl - \check{Cl} \|, \| Cr - \check{Cr} \|\right)}{\| Cl - Cr \|} \tag{6}$$

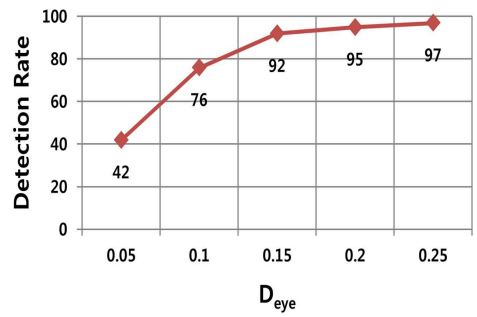

Fig. 4: Experiment result for pupil center detection using BioID DB

Here, D_{eye} means the error in the result, and each test was performed with accepted error rate ranges until 0.05, 0.1, 0.15, 0.2, and 0.25. Next, $Cl, \check{Cl}$ and $Cr, \check{Cr}$ denote the pupil center detected in the exact center point of each eye (left and right) in BioID DB and the pupil center detected in the experiment. Fig. 4 shows the experimental result.

3.2 Gaze Direction

Since human gaze direction can be estimated by detecting the pupil center in the real time basis, we present a system that detects the current gaze direction using the exact pupil center and distance of the vertical and horizontal sclera. First, to reduce error in detecting the pupil center, average distance between pupils is measured within the 20 frames acquired in the real time base, while excluding the distance with the largest variance in the pupil distance. The average distance is compared with the detected distance between pupils to determine the accuracy of current detection. Second, the distance of vertical and horizontal sclera is calculated with the detected pupil at the center. To reduce error, unnecessary region is removed based on the skin color. The removed region is changed to black and the distance in bright region of the sclera is calculated to detect the current gaze detection. Fig. 5 shows the result for the gaze detection task. The pictures above show how the gaze direction is detected. However, when the person is looking downward, the pupil is hidden and it becomes difficult to detect them. The frequency of change in gaze direction is analyzed and drowsiness is determined when there is no change in about 200 frames.

3.3 Blink Detection

In this section, we describe how to detect the eye blink. It is known when human gets drowsy, the blood is moving to the end of hands and feet, and the eyes are blinked more often because tear production in the lachrymal glands is reduced. In addition, the blood supply to the

© 2015 NSP
Natural Sciences Publishing Cor.

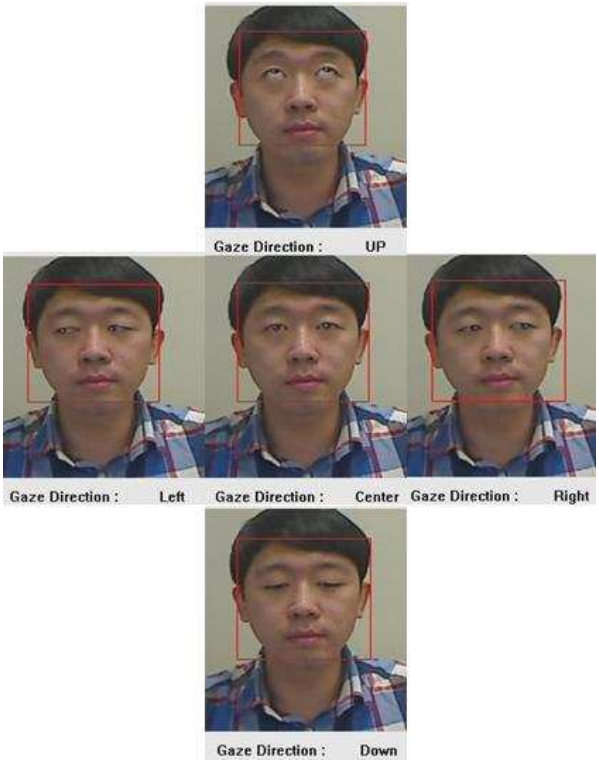

Fig. 5: Result of gaze direction detection experiment

brain is also reduced. As a result of these, the person goes into a trance state as the brain activity is naturally reduced. The eye region of a human is usually darker than facial skin. We determine whether eyes are opened or closed by using that information, called Integral Projection Function (IPF). First, the pupil area is designated based on the above pupil center point. However, it is important not to include the eyebrows when designating the pupil region because it may affect the binarization operation. In addition, histogram equalization is carried out for the pupil area as shown in Fig. 6(A). This image is binarized using a threshold of the dark color and then processed a morphology operation. Through this, the eye region within the given image can be extracted as shown in Fig. 6(B). Finally, the characteristics of pupil region are detected through IPF as shown in Fig. 6(C). Here, an arbitrary area is designated proportionally in the maximum value in the IPF image. Then, an error is obtained by comparing the ratio and size of the dark area within the designated area and a blink is detected with this. The ratio of the arbitrary area was 0.5. Eye blinking was detected by using IPF image obtained using this method.

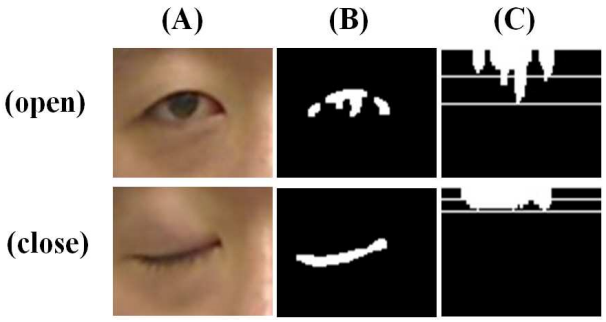

Fig. 6: IPF varies depending on opening and closing of the eyes, (A) Input images, (B) The binarized images, (C) The IPF images

3.4 Blink Detection Result

In order to evaluate the performance of our eye blink detection algorithm, we have recorded natural eye blinking of the human subjects using a Webcam. The recording frequency of the video was 30f/s and the total frame was 600. Fig. 7 illustrates the result for the performance analysis.

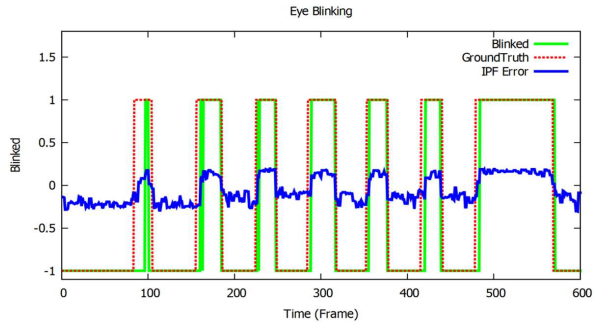

Fig. 7: Blink detection result

The blue line in the Fig. 7 represents the IPF error values. To account the one-eye close, such as making a wink, they are calculated for both eyes and only the average values are shown here. The red dot line shows the ground-truth values. The green line indicates the blink detection results using the present system. When the error value is greater than zero, the eyes of the subject are closed. The averaged blink detection rate reaches to 92%.

4 Driver Drowsiness Detection

Since our final goal is to determine driver's drowsiness using several drowsiness-related parameters presented above sections, we need a driver database that should be collected from a vehicle environment. However, it is not

© 2015 NSP
Natural Sciences Publishing Cor.

easy to collect such data simply because it could be very dangerous to manage sleepy drivers in the moving car. One possible solution is to let the subject drivers to simulate drowsy driver in the vehicle according to a certain scenario containing several drowsiness behaviors.

4.1 Driver Video Production

Two scenarios are prepared: the normal driving and the drowsy driving. For the former, the subject supposes to look at the side and rear mirrors sporadically with a normal attentive forward viewing and yet to drive with natural blinking. For the later, the subject blinks often like a drowsy driver and his head tends to lock in a certain head direction without looking at the side and rear mirrors. During the whole recording session, each subject wears a gyro sensor module mounted in a white box that is again attached to a black head-band as shown in Fig. 8(Left). The sensor is responsible to measure 3D head-movement of the driver, and the collected data are sent in the real-time basis to the receiver, which connects to a PC within the vehicle, using the wireless communication protocol. This setup allows each subject focusing only on a given scenario, resulting in improved usability comparing to the previous studies [2]. Table 3 summarizes specifications of the wireless gyro-sensor module.

Fig. 8: Wireless Gyro-sensor module mounted in a white box and its receiver (Left) and cameras and other setup installed in the vehicle (Right)

Table 3: Specification of the gyro sensor module

Wireless Frequency (GHz)	2.4
Degree of Freedom & Sensor Type	9 axis MEMS
Sensitivity (dps)	250 2000
Accelerator Sensitivity (G)	2 16

We have collected two stream of videos concurrently using two cameras: one for the color image and the other for black and white image. The former is used for the basis, whereas the later works with an IR (Infra-Red) LED panel to dealing with the night vision. Each video was collected by synchronizing with the gyro-sensor. Fig. 8(Right) shows the whole setup installed in front of the driver hand in the vehicle. And Fig. 9 provides some samples images taken under the dim illumination condition.

4.2 Determiantion of Driver Drowsiness using Several Factors

In this section, we show how to determine driver drowsiness by combining three different factors: Head-pose movement, gaze direction and eye blinking data. First, the head-pose of driver is one of important factor in determining drowsiness. One may guess that drowsy drivers simply nodes his head regularly. However, if someone nodes his head, he is already in the sleeping mode, resulting a car clash. In fact, when a driver is drowsy, initially his head tends not moving very much and vigilance of looking at the side and back mirrors is impaired. It is known that the largest proportion of truck drivers accidents dues to drowsy driving. In particular, many of them occur on a straight road such as highways driving long time. In such circumstance, the head of the driver is initially not moving very much and then the nodding behavior occurs just before the accident.

Fig. 9: Sampled images from the collected videos with the dim illumination condition. Color images (Top), Gray images (Bottom) taken under the IR illumination

To prevent such car accident in the early stage, it seems reasonable to measure the ratio of non-moving head-pose state. It can be calculated for 50 frames to use in detecting drowsiness of the driver. Equation 7 shows this:

$$S_{HP} = \sqrt{\frac{1}{49}\sum_{i=f}^{f+50}(HP_i - \bar{HP})^2} \tag{7}$$

© 2015 NSP
Natural Sciences Publishing Cor.

Table 4: Determination of Drowsy Driving

	Head Pose	**Gaze Direction**	**Blink**
Evaluation method	Standard Deviation(S_{HP})	Standard Deviation(S_{GD})	PERCLOS
Detection criteria	Immovable	Immovable	Increased blinking
Ratio of two cases (%)	50%	50%	
Drowsiness determination	Drowsiness level $\geq$ 80%		

Here, HP represents the head-pose data (Yaw, Pitch and Roll) and $\overline{HP}$ does the average of HP. Then, S_{HP} can be an evaluation criterion how much the head of the driver is not moving. As this value is closer to zero, the degree of drowsiness is high. In addition, gaze direction tracking and blink are also used in determining drowsiness of driver. It is known that PERCLOS is the most appropriate method in determining the eye blinking state. Since PERCLOS is normally obtained by calculating the ratio of closing the eyes for 5 seconds, we measure the frames of closed-eye during 150 frames as the recording frequency of our camera is 30 f/s. Later, we calculate PERCLOS by adding the standard deviation of gaze direction. The reason of using both gaze direction and blinking is that it is difficult to detect gaze during closing your eyes. Equation 8 shows this:

$$PERCLOS = \frac{N_c}{150} + S_{GD} \tag{8}$$

Here, N_C represents the number of eyes closed and S_{GD} the standard deviation of gaze direction.

The drowsy level of the subject is determined by combining PERCLOS and standard deviation of the head-pose state. When the drowsy level is more than 80%, a certain kind of warning will be given to the driver. Table 4 summarizes the methods we have used and their evaluation criteria.

The drowsy level of the subject is determined by combining PERCLOS and standard deviation of the head-pose state. When the drowsy level is more than 80%, a certain kind of warning will be given to the driver. Table 4 summarizes the methods we have used and their evaluation criteria.

4.3 Experiment Result

In this section, we present the result of performance evaluation of our method using the driver database we have constructed. In Fig. 10 the graphs in the left are for the fresh driver and those in the right are for the drowsy driver. The top two graphs show the estimation result of the head pose movement for the fresh driver and the drowsy driver, respectively. The former looks at the side-view and the rea-view mirror sporadically, whereas the later keeps looking at a certain direction. The sudden change in the pitch movement in the end indicates the nodding of his head. The middle two graphs show PERCLOS with the gaze direction of the subject. It is known that humans make 15 to 20 times of eye blinking per minute. In case of the fresh driver, the ratio of PERCLOS graph is less 0.2 because his gaze direction changes continuously and his eye blinking is also normal. However, the drowsy driver shows the high ratio of PERCLOS because gaze direction does not change very much and his eye blinking increases. The bottom graphs illustrate the drowsiness levels by combining above two parameters: PERCLOS and Head-pose movement. When the drowsiness level is over 80%, the system tells that the driver is drowsy. Our result suggests the drowsiness level of the fresh driver is normally less than 50% and that of the drowsy driver is more than 90%.

5 Conclusion

This paper presents a drowsy-driver detection system in which the head pose, gaze direction and eye blink of the driver are measured in the real-time basis and the level of drowsiness is determined by combining those parameters. It seems that such data fusion allows us having a reliable drowsy-driver detection system, because it is very difficult to judge whether a driver is sleepy or not if we depend on only one behavior pattern. Since the drowsy driver often yawns, we plan to add it our system in the near future.

Acknowledgements

This research was supported by Basic Science Research Program through the National Research Foundation of Korea (NRF-2013R1A1A2006969) and by IT/SW Creative Research Program through the National IT Industry Promotion Agency (NIPA-2013-H0502-13-1019).

References

[1] T. A. Ranney, E. Mazzae, R. Garrot, and M. J. Goodman, ”NHTSA driver distraction research: Past, present, and future,” Nat. Highway Traffic Safety Admin., East Liberty, OH, USA, Tech. Rep., 2000.

[2] DeMenthon and L. S. Davis, ”Model-based object pose in 25 lines of code,” Int. J. Comput. Vis., **15**, 123–141, 1995.

[3] M. La Cascia, S. Sclaro, and V. Athitsos, ”Fast, reliable head tracking under varying illumination: An approach based on registration of texturemapped 3D models”, IEEE Trans. Pattern Anal. Mach. Intell.,**22**, 322–336, 2000.

[4] R. Oyini Mbouna, S. G. Kong, and M-G. Chun, ”Visual Analysis of Eye State and Head Pose for Driver Alertness Monitoring”, IEEE Trans. Intelligent Transportation Systems, **14**, 1462–1469, 2013

© 2015 NSP
Natural Sciences Publishing Cor.

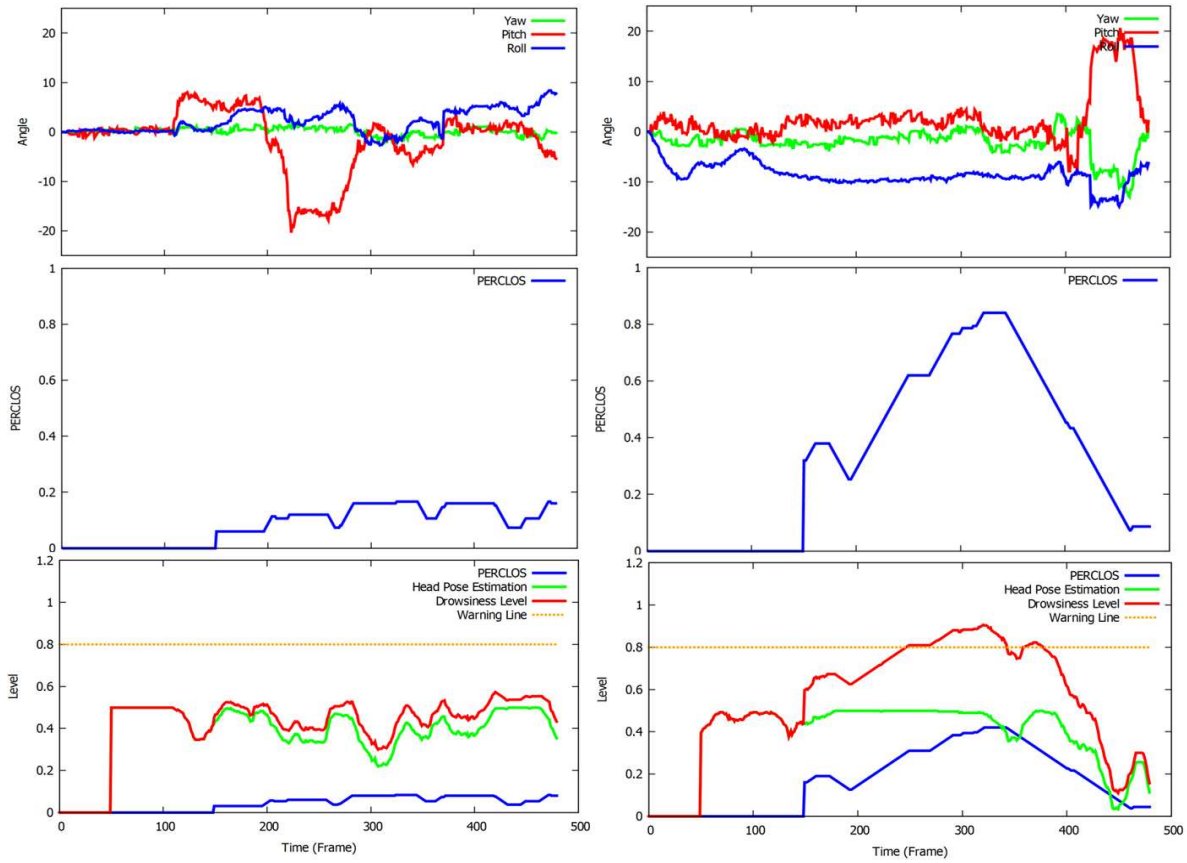

Fig. 10: Result of driver drowsiness detection for the fresh driver(Left Column) and the drowsy driver(Right Column). The top row shows the head pose estimation. The middle PERCLOS and the bottom the decision of the drowsiness level, respectively

[5] O. Jesorsky, K. Kirchberg, and R. Frischholz, "Robust face detection using the Hausdorff distance," in Proc. Audio Video Based Biometric Person Authentification, **3**, 90–95 , 2001.
[6] Z. Zhou and X. Geng, "Projection functions for eye detection," Pattern Recognit., **37**, 1049–1056, 2004.
[7] M. Asadifard and J. Shanbezadeh, "Automatic adaptive center of pupil detection using face detection and CDF analysis," in Proc. Int. MultiConf. Eng. Comput. Scientists, **1**, 130–133, 2010.
[8] D. F. Dinges and R. Grace, "PERCLOS: A valid psychophysiological measure of alertness as assessed by psychomotor vigilance," Fed. Highway Admin., Washington, DC, USA, Tech. Rep., 1998.
[9] R. Wang., G. Lie, B, Ting., & L. Jun.. "Monitoring mouth movement for driver fatigue or distraction with one camera," In Intelligent Transportation Systems, Proceedings. The 7th International IEEE Conference, 314–319. 2004.
[10] Singular Inversion, I. FaceGen. http://www.facegen.com.

In-Ho Choi received his Master Degree from Sejong University and is currently a PhD candidate in the Department of Computer Engineering. His research interests are facial expression recognition and driver safety system.

Yong-Guk Kim received his PhD degree from Cambridge University. He is currently a Full Professor with the Department of Computer Engineering, Sejong University, Seoul Korea. His research interests are facial expression recognition and synthesis, computational vision, and human-computer interaction.

© 2015 NSP
Natural Sciences Publishing Cor.